CHAPTER 4 RESULTS AND DISCUSSION

4.1 PEM fuel cell dynamic model

The model of proton exchange membrane fuel cell (PEMFC) is considered to the mass transfer in the anode/cathode channel, and the energy transfer in the fuel cell stack. The establishment of a lumped-parameter dynamic model is realized using a combination of intrinsic mechanistic relations and empirical modeling. The dynamic models are developed based on the controlled (hydrogen and oxygen partial pressure, and stack temperature), manipulated (hydrogen, oxygen and cooling water flowrate) and disturbance (current load) variables of the system.

Since the dynamic models of PEMFC from Equations 3.1-3 are the non-linear model, linearization by using Taylor's series expansion is necessary before generating the state space of the PEMFC system. The linear dynamic models of PEMFC are presented as the following:

$$\frac{dP'_{H_2}}{dt} = \frac{R}{V_{an}}[\dot{m}_{H_2,in} - k_{an}(P^{\circ}_{H_2} - P_{H_2,in}) - \frac{NI^{\circ}}{2F}]T'_s - [\frac{k_{an}RT^{\circ}_s}{V_{an}}]P'_{H_2} + [\frac{RT^{\circ}_s}{V_{an}}]\dot{m}'_{H_2,in} - [\frac{RT^{\circ}_s N}{2FV_{an}}]I' \quad (4.1)$$

$$\frac{dP'_{O_2}}{dt} = \frac{R}{V_{cat}}[\dot{m}_{O_2,in} - k_{cat}(P^{\circ}_{O_2} - P_{O_2,out}) - \frac{NI^{\circ}}{4F}]T'_s - [\frac{k_{cat}RT^{\circ}_s}{V_{an}}]P'_{O_2} + [\frac{RT^{\circ}_s}{V_{an}}]\dot{m}'_{O_2,in} - [\frac{RT^{\circ}_s N}{4FV_{cat}}]I' \quad (4.2)$$

$$\frac{dT'_s}{dt} = \frac{1}{c_t}[-K_{conv,amb} - \frac{\dot{m}_{cw}C_{pw}Mw_{H_2O}}{1000}]T'_s + \frac{1}{c_t}[\frac{-C_{pw}Mw_{H_2O}(T_s - T_c)}{1000}]\dot{m}'_{cw} + \frac{1}{c_t}[\frac{N\Delta H}{2F} - V_{stack}]I' \quad (4.3)$$

4.2 PEM fuel cell passive model

To study the transient response of proton exchange membrane fuel cell (PEMFC) by using the passivity concept, the linear dynamic model of PEMFC is first represented in the state-space form. Arranging Equations 4.1-3 in state space form to find out the transfer function of the system as following:

$$\begin{bmatrix} \dot{P}_{H_2} \\ \dot{P}_{O_2} \\ \dot{T}_s \end{bmatrix} = \begin{bmatrix} A_{11} & 0 & A_{13} \\ 0 & A_{22} & A_{23} \\ 0 & 0 & A_{33} \end{bmatrix} \begin{bmatrix} P_{H_2} \\ P_{O_2} \\ T_s \end{bmatrix} + \begin{bmatrix} B_{11} & 0 & 0 \\ 0 & B_{22} & 0 \\ 0 & 0 & B_{33} \end{bmatrix} \begin{bmatrix} \dot{m}_{H_2,in} \\ \dot{m}_{O_2,in} \\ \dot{m}_{cw} \end{bmatrix} + \begin{bmatrix} E_{11} \\ E_{21} \\ E_{31} \end{bmatrix} [I]$$

$$\begin{bmatrix} P_{H_2} \\ P_{O_2} \\ T_s \end{bmatrix} = \begin{bmatrix} 1 & 0 & 0 \\ 0 & 1 & 0 \\ 0 & 0 & 1 \end{bmatrix} \begin{bmatrix} P_{H_2} \\ P_{O_2} \\ T_s \end{bmatrix} \qquad D = [0] \quad (4.4)$$

where $A_{11} = -\frac{k_{an}RT^{\circ}_s}{V_{an}}$ $\qquad A_{13} = \frac{R}{V_{an}}[\dot{m}_{H_2,in} - k_{an}(P^{\circ}_{H_2} - P_{H_2,in}) - \frac{NI^{\circ}}{2F}]$

$$A_{22} = -\frac{k_{cat} RT_s^{\circ}}{V_{an}} \qquad A_{23} = \frac{R}{V_{cat}}[\dot{m}_{O_2,in} - k_{cat}(P_{O_2}^{\circ} - P_{O_2,out}) - \frac{NI^{\circ}}{4F}]$$

$$A_{33} = \frac{1}{c_t}[-K_{conv,amb} - \frac{\dot{m}_{cw} C_{pw} Mw_{H_2O}}{1000}]$$

$$B_{11} = \frac{RT_s^{\circ}}{V_{an}} \qquad B_{22} = \frac{RT_s^{\circ}}{V_{an}}$$

$$B_{33} = \frac{1}{c_t}[\frac{-C_{pw} Mw_{H_2O}(T_s^{\circ} - T_c)}{1000}]$$

$$E_{11} = -\frac{RT_s^{\circ} N}{2FV_{an}} \qquad E_{21} = -\frac{RT_s^{\circ} N}{4FV_{cat}} \qquad E_{31} = \frac{1}{c_t}[\frac{N\Delta H}{2F} - V_{stack}^{\circ}]$$

After substituting the numerical values at steady-state into A,B,C and E constant matrixes which can be illustrated in Appendix A, the state space of PEMFC system is represented as the following:

$$\begin{bmatrix} \dot{P}_{H_2} \\ \dot{P}_{O_2} \\ \dot{T}_s \end{bmatrix} = \begin{bmatrix} -0.3712 & 0 & 0 \\ 0 & -0.1856 & 0 \\ 0 & 0 & -0.0028 \end{bmatrix} \begin{bmatrix} P_{H_2} \\ P_{O_2} \\ T_s \end{bmatrix} + \begin{bmatrix} 5.7106 & 0 & 0 \\ 0 & 2.8553 & 0 \\ 0 & 0 & -0.2096 \end{bmatrix} \begin{bmatrix} \dot{m}_{H_2,in} \\ \dot{m}_{O_2,in} \\ \dot{m}_{cw} \end{bmatrix} + \begin{bmatrix} -0.001 \\ -0.0003 \\ 0.0014 \end{bmatrix} [I]$$

$$\begin{bmatrix} P_{H_2} \\ P_{O_2} \\ T_s \end{bmatrix} = \begin{bmatrix} 1 & 0 & 0 \\ 0 & 1 & 0 \\ 0 & 0 & 1 \end{bmatrix} \begin{bmatrix} P_{H_2} \\ P_{O_2} \\ T_s \end{bmatrix} \qquad D = [0] \tag{4.5}$$

To analyze the characteristic of PEMFC system, the transfer function of PEMFC system including the transfer function of disturbance are find out by using Equations refer from 2.21-22.

$$G_p(s) = C(sI - A)^{-1} B + D \tag{2.21}$$

$$G_d(s) = C(sI - A)^{-1} E \tag{2.22}$$

where

$$A = \begin{bmatrix} -0.3712 & 0 & 0 \\ 0 & -0.1856 & 0 \\ 0 & 0 & -0.0028 \end{bmatrix} \qquad B = \begin{bmatrix} 5.7106 & 0 & 0 \\ 0 & 2.8553 & 0 \\ 0 & 0 & -0.2096 \end{bmatrix}$$

$$C = \begin{bmatrix} 1 & 0 & 0 \\ 0 & 1 & 0 \\ 0 & 0 & 1 \end{bmatrix} \qquad D = [0] \qquad E = \begin{bmatrix} -0.001 \\ -0.0003 \\ 0.0014 \end{bmatrix}$$

By using Matlab, the matrix transfer functions can be determined as following:

$$\text{Process:} \quad \begin{bmatrix} P_{H_2} \\ P_{O_2} \\ T_s \end{bmatrix} = \begin{bmatrix} \dfrac{5.711}{s+0.3712} & 0 & 0 \\ 0 & \dfrac{2.855}{s+0.1856} & \dfrac{1.182\times10^{-17}}{s^2+0.1884s+0.0005277} \\ 0 & 0 & \dfrac{-0.2096}{s+0.002843} \end{bmatrix} \begin{bmatrix} \dot{m}_{H_{2,in}} \\ \dot{m}_{O_{2,in}} \\ \dot{m}_{cw} \end{bmatrix} \tag{4.6}$$

$$\text{Disturbance:} \quad \begin{bmatrix} P_{H_2} \\ P_{O_2} \\ T_s \end{bmatrix} = \begin{bmatrix} \dfrac{-0.001036}{s+0.3712} \\ \dfrac{-0.0002589s-2.362\times10^{-7}}{s^2+0.1884s+0.0005277} \\ \dfrac{0.001416}{s+0.002843} \end{bmatrix} [I] \tag{4.7}$$

From Equations 4.6-7, there are three loop controls in this work ($\dot{m}_{H_{2,in}} - P_{H_2}$, $\dot{m}_{O_{2,in}} - P_{O_2}$ and $\dot{m}_{cw} - T_s$) and one disturbance variable (I). After the transfer function of the process and disturbance are obtained from Matlab, passivity index is employed to analyze how far of PEMFC system is being passive. The passivity index of PEMFC system is illustrated in Figure 4.1.

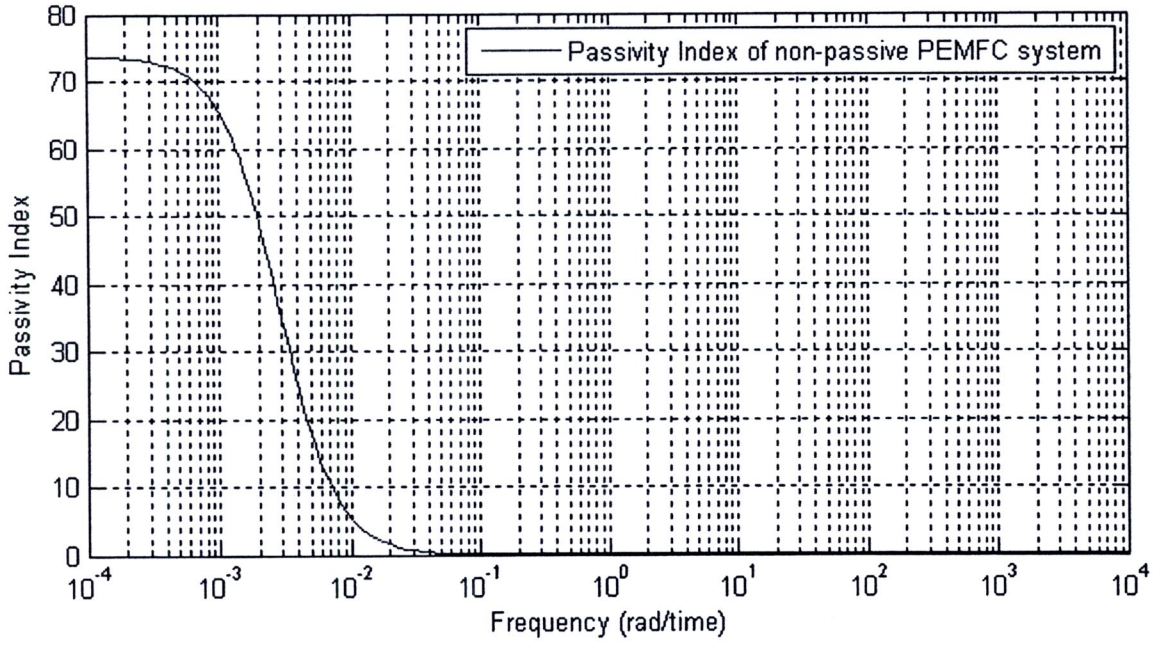

Figure 4.1 The passivity index of non-passive PEMFC system

Figure 4.1 shows that the PEMFC system is non-passive due to a positive value of passivity index. According to the passivity concept, the non-passive process can be

shifted to the passive process by adding the stable and minimum phase transfer function matrix $w_p(s)$, which is called weighting function. The result of the weighting function after solving Problem 1 that make the PEMFC system shift into the passive system is presented following:

$$w_p(s) = \frac{1.s.(s+35.924)}{(s+1.268\times10^{-7}).(s+0.311)} \tag{4.8}$$

The weighing function from Equation 4.8 is added to the transfer function of PEMFC system as presented by Equation 2.27, $H(s) = G(s)U + w_p(s)I$. Then the non-passive PEMFC system shifts to the passive system, the passivity index of passive system is illustrated in Figure 4.2.

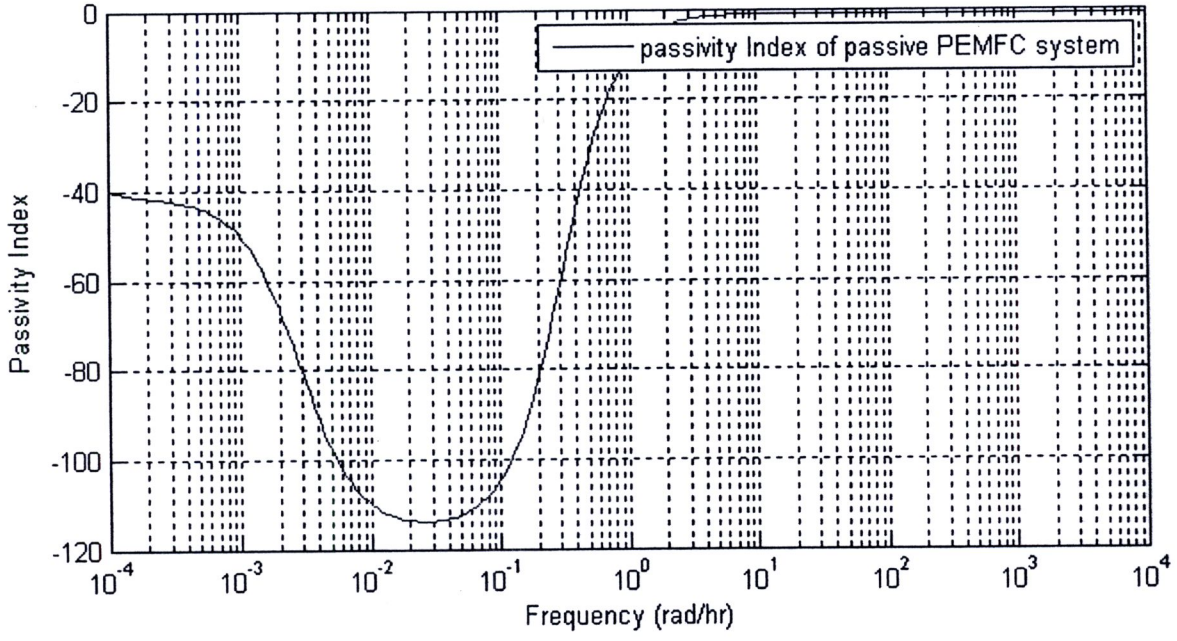

Figure 4.2 The passivity index of passive PEMFC system

Figure 4.2 shows a negative value of the passivity index that means the system is passive system. However, the weighting function cannot be added into the system directly because the system cannot change [22]. Therefore, the weighting function will be absorbed into the controller to design the passive controller for using in the PEMFC system.

4.3 PEM fuel cell passive controller

Based on the passivity concept, the feedback system comprises of a passive system and a strictly passive system is asymptotically stable. In this work, the PEMFC is already shifted to strictly passive system, therefore, the passive controller for each loop control is designed to make the PEMFC system is asymptotically stable.

The passive controllers with integral action (PI controller) are designed from the optimization problem 2. The results of the $k_{c,i}^{+}$ and $\tau_{I,i}$ for each loop control are shown in Table 4.1.

Table 4.1 The results of the $k_{c,i}^{+}$ and $\tau_{I,i}$ for each loop control

	Loop No.	$k_{c,i}^{+}$	$\tau_{I,i}$ (second)
1.	$\dot{m}_{H_2,in} - P_{H_2}$	0.001	20
2.	$\dot{m}_{O_2,in} - P_{O_2}$	0.001	20
3.	$\dot{m}_{cw} - T_s$	0.001	12

From Table 4.1, noticing, the value of $\tau_{I,i}$ for each loop control is very small. The result shows that by solving the optimization problem 2, the controllers will fast response when the disturbance or other input variables changed are applied to the PEMFC system.

Since the controllers used in multi-control system are PI controller, the values of $k_{c,i}^{+}$ and $\tau_{I,i}$ from Table 4.1 are plugged in the simple form of PI controller as follow:

$$k_i^{+} = k_{c,i}^{+}\left(1+\frac{1}{\tau_{I,i}s}\right) \tag{4.9}$$

By substituting the values from Table 4.1, the result for k_i^{+} of each loop control are shown in the following.

$$k_1^{+} = 0.001\left(1+\frac{1}{20s}\right) \quad \text{for the control loop} \quad \dot{m}_{H_2,in} - P_{H_2}$$

$$k_2^{+} = 0.001\left(1+\frac{1}{20s}\right) \quad \text{for the control loop} \quad \dot{m}_{O_2,in} - P_{O_2}$$

$$k_3^{+} = 0.001\left(1+\frac{1}{12s}\right) \quad \text{for the control loop} \quad \dot{m}_{cw} - T$$

Based on the passivity concept, the close-loop system will be stable when the weighting function is absorbed into the controller. The passive controller is designed by recall Equation 2.36.

$$k_i^{'}(s) = k_i^{+}(s)[1 - w_p(s)k_i^{+}(s)]^{-1} \tag{2.36}$$

After substituting k_i^{+} and $w_p(s)$ into Equation 2.36, the controller transfer function of each loop control after neglecting some useless terms can be determined as follow:

$$k_1'(s) = \frac{20s^3 + 7.22s^2 + 0.311s}{2\times10^4 s^2(s+0.275)} \tag{4.10}$$

$$k_2'(s) = \frac{20s^3 + 7.22s^2 + 0.311s}{2\times10^4 s^2(s+0.275)} \tag{4.11}$$

$$k_3'(s) = \frac{12s^3 + 4.74s^2 + 0.311s}{1.2\times10^4 s^2(s+0.275)} \tag{4.12}$$

These three passive controllers will be used in the closed-loop PEMFC system.

4.4 PEM fuel cell model verification

The developed PEMFC model is integrated of all possible dynamic equations by including the dynamic models of lump fuel cell body, anode and cathode channels. This model is developed for capturing the transient responses of the cell voltage (V_{stack}), the stack temperature (T_s), the hydrogen and oxygen input flowrates ($\dot{m}_{H_2}, \dot{m}_{O_2}$) and the hydrogen and oxygen partial pressure in anode and cathode channels (P_{H_2}, P_{O_2}) including the membrane humidity (RH) under sudden change in the load current (I). The dynamic model is implemented using Simulink as shown in Figure 4.3.

In Figure 4.3, there are three inputs ($\dot{m}_{H_2}, \dot{m}_{O_2}, \dot{m}_{cw}$) and three outputs ($P_{H_2}, P_{O_2}, T$) with one disturbance ($I$). In this part of study, the developed PEMFC model is verified by comparing with the results of Wu et al. [9], based on the 5kW Ballard stack. To verify the model performance, the current load which is the disturbance variable of this work is step changed from 100 A to 250 A similar to Wu et al. work. The results of the voltage profile, the stack temperature profile, and the hydrogen/oxygen partial pressure profile including the power of PEMFC system are shown in Figure 4.4.

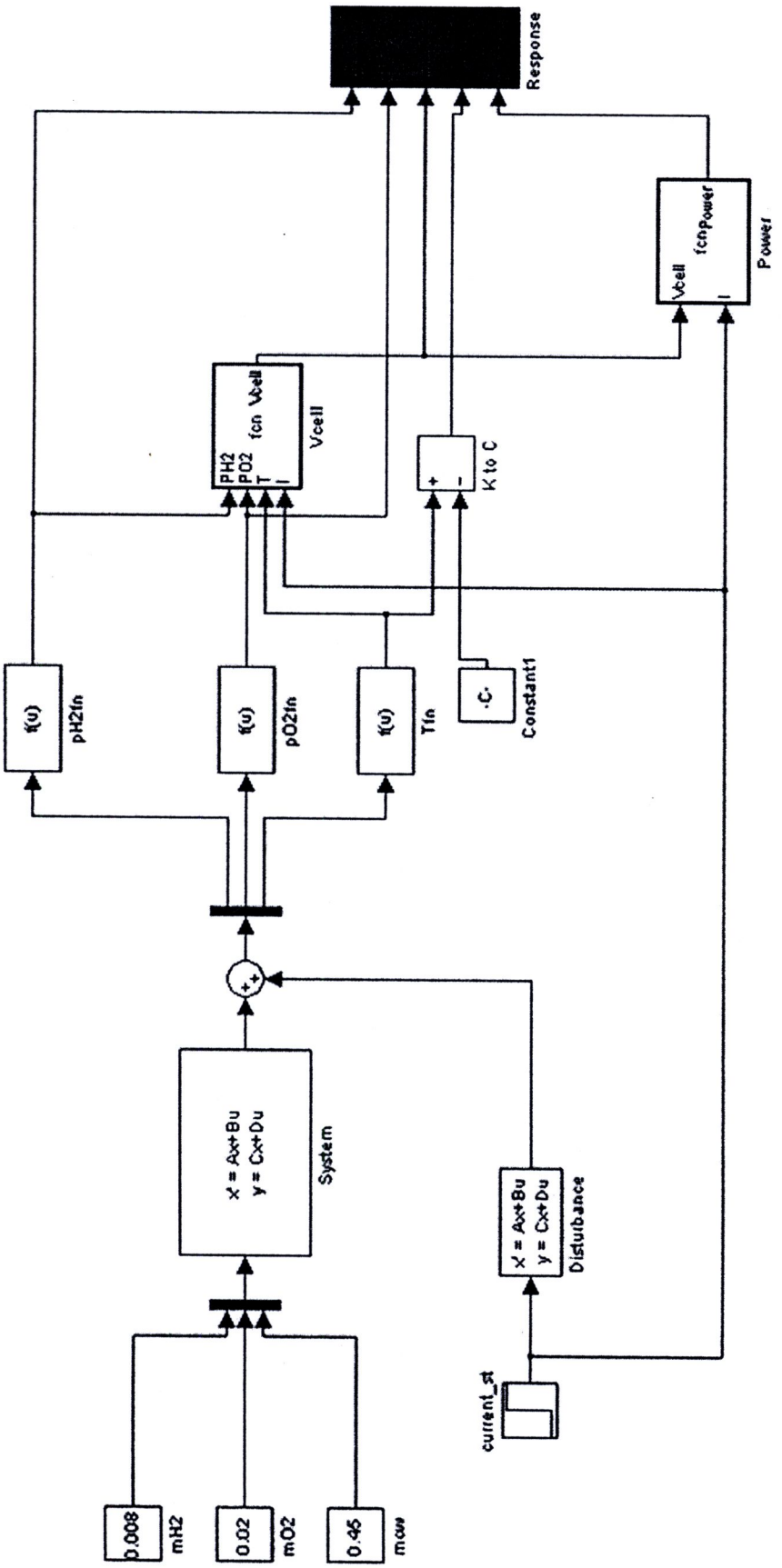

Figure 4.3 The PEMFC model without controller

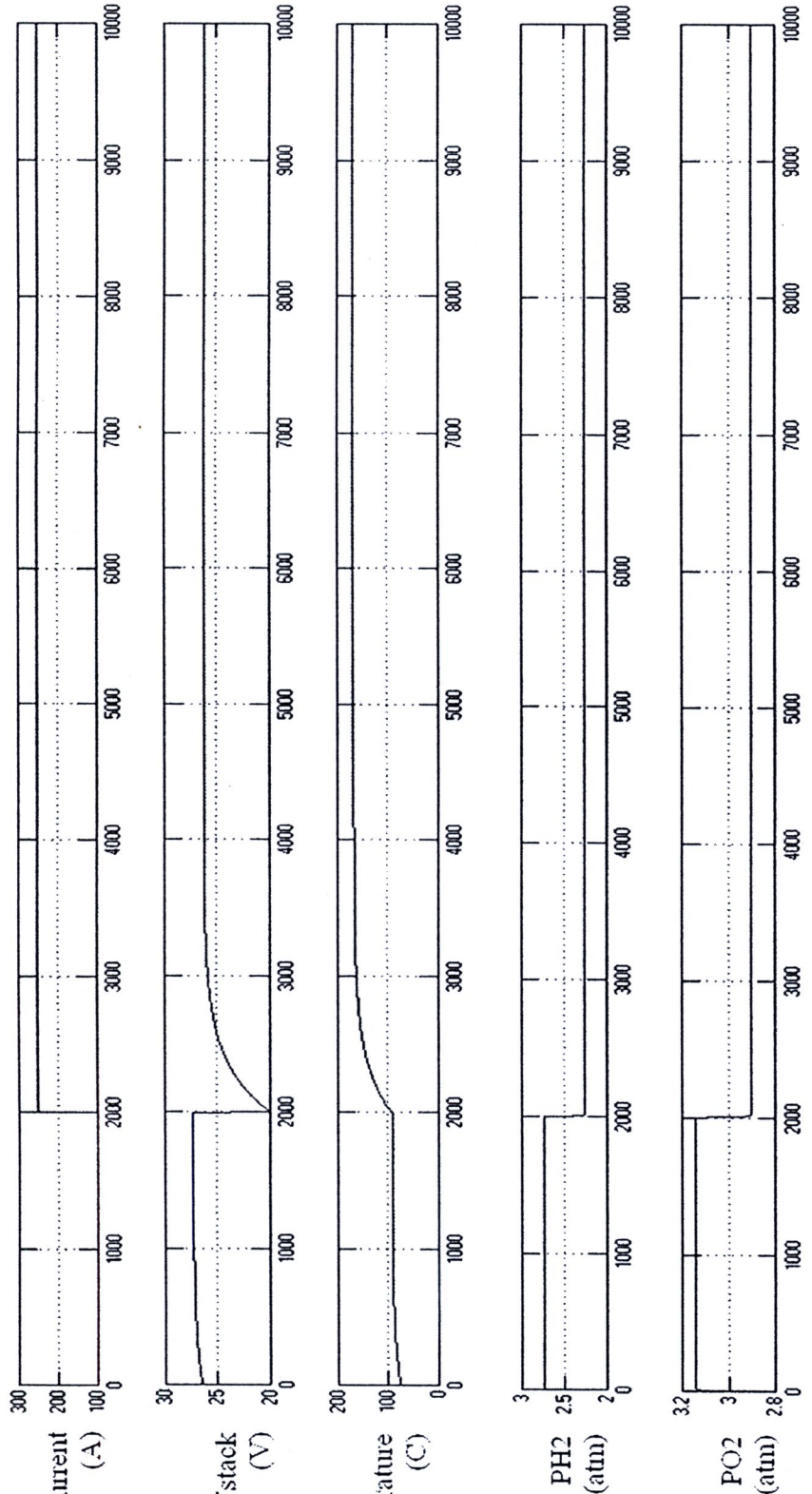

Figure 4.4 The transient response of V_{stack}, T_s, P_{H_2} *and* P_{O_2} after step change I from 100A to 250A without controller

From Figure 4.4, after step change of the load current from 100 A to 250A at time 2,000 seconds, the hydrogen and oxygen partial pressure in the channels decrease suddenly to their new steady state (2.25 and 2.9 atm) due to an increasing of reactants consumption for supporting an increasing of the electrochemical reaction. Since the reaction which is an exothermic reaction increases, the amount of waste heat produced at higher current causes the stack temperature to increase (T_s=175°C) resulting in an increasing in the cell voltage due to the decreasing of internal cell resistance. Noticing, there is high voltage drops at the time which the load current suddenly steps up, this is due to an increasing of the ohmic voltage resistance from the higher current step changes. However, although, the cell voltage increases slowly again after the current load steps up at time 2,000 seconds, it still lower than 27.5 Volt, which is the value of it steady state before the PEMFC is disturbed by the current load. This phenomenon will give the low performance of PEMFC. The profiles of the transients in V_{stack}, T_s, P_{H_2} *and* P_{O_2} depicted in Figure 4.4 from this model are similar to that of Wu et al. [9] model. This shows that this model under identical conditions accurately predicts the system behavior.

4.5 Multi-loop control system

Due to the previous section, the step up of load current causes an increasing in stack temperature and decreasing in the net output voltage. Normally, the PEMFC can work well at the stack operating temperature between 70-100°C. Since the stack temperature becomes too high $(T_s > 100^{\circ}C)$, PEMFC may be damaged from membrane drying out. In addition, if the cell voltage becomes too low, the electrode catalyst becomes exposed to possible damage. To address these two issues, the decentralized passive controllers with integral action (PI controller) are designed in order to control both the stack temper and the cell voltage under the disturbance is applied to PEMFC.

4.5.1 Temperature and voltage control

In this work, the decentralized passive controllers are designed by using the passivity concept. As the passivity concept state that if the multi-variable process system $G(s)$ is strictly passive, then the closed-loop system will be stable if the multi-loop controller $K(s)$ is passive. For PEMFC system, the process renders strictly passive and the controller renders passive by absorbing the minimum phase transfer function $(w_p(s))$, therefore, this system become stable. The stability of PEMFC system is verified with the loop fails and the disturbance. The disturbance variable for this study is the +50A increasing of the current load at time 10,000 seconds, and -30A decreasing at time 40,000 seconds. Figure 4.5 shows the closed-loop of PEMFC system with controller.

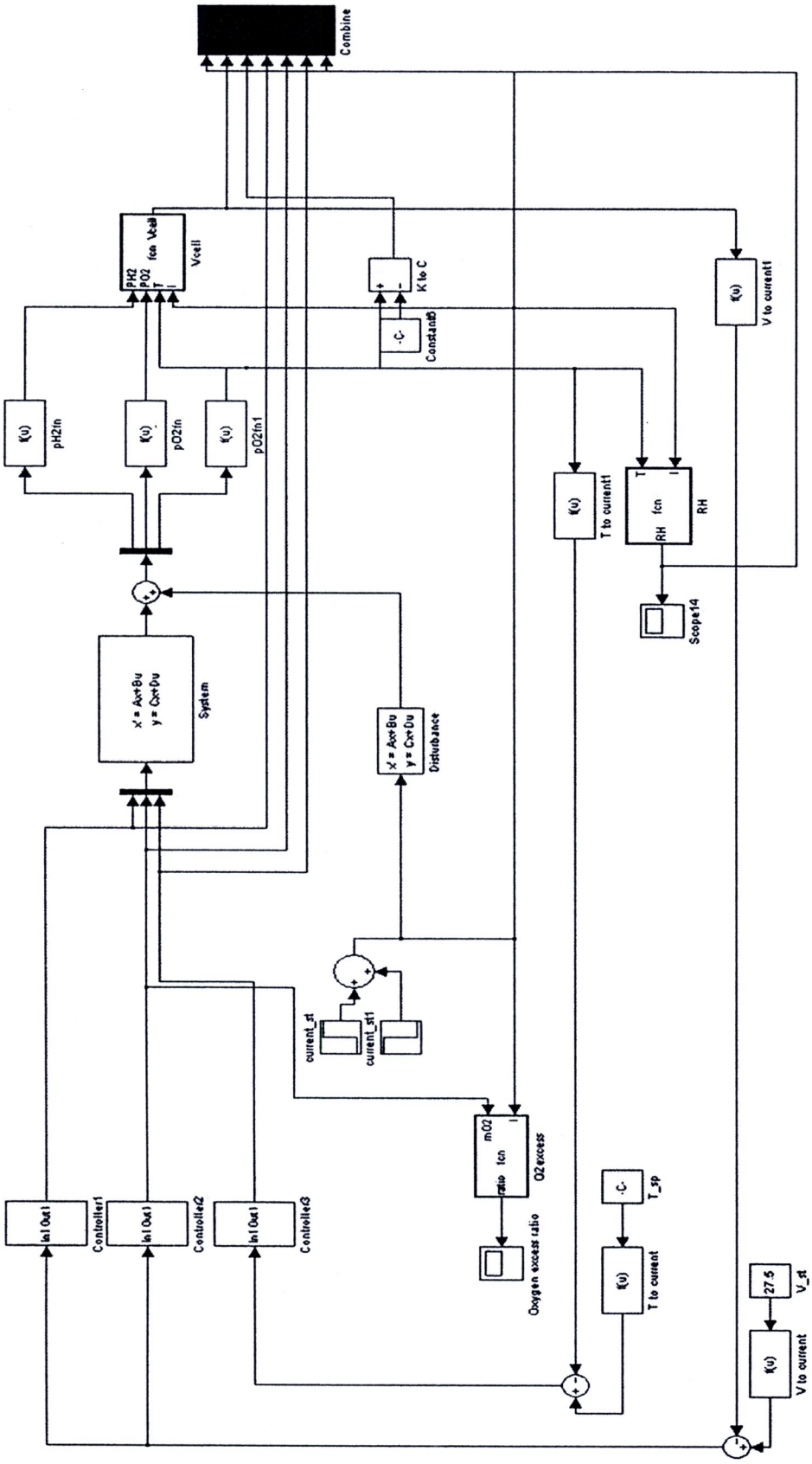

Figure 4.5 The PEMFC model with controllers (T_s *and* V_{stack} control)

In Figure 4.5, there are three passive controllers, one for temperature control ($k_3^{'}$) by manipulating the cooling water flowrate ($\dot{m}_{cw} - T$), and the others for voltage control ($k_1^{'}$ *and* $k_2^{'}$) by manipulating the hydrogen and oxygen flowrates ($\dot{m}_{H_2}, \dot{m}_{O_2}, -V_{stack}$). In this work, the hydrogen and oxygen flowrates are directly effect to the hydrogen and oxygen partial pressure. Hydrogen and oxygen partial pressures are then directly effect to the cell voltage, therefore we can control the cell voltage by manipulating the hydrogen and oxygen flowrates. The set point of the cell voltage and the stack temperature are set up at their steady state before they are disturbed by the disturbance, 27.5 Volt and 90°C, respectively. After the current load is applied to the process, the transient responses with temperature-voltage controllers are presented in Figure 4.6.

During time 0-10,000 seconds, all control variables maintain at their steady state. After that, the current load steps up from 100A to 150A. The cell voltage suddenly decreases and the stack temperature suddenly increases more than 100°C. As the result, the controllers ($k_1^{'}$ *and* $k_2^{'}$) manipulate the hydrogen and oxygen flowrates by increasing their flowrates (0.45 mol/s for hydrogen, and 0.6 mol/s for oxygen) to maintain the cell voltage at 27.5 Volt, and the controller ($k_3^{'}$) will increase the cooling water about 1 mol/s to cool the stack temperature down and maintain at 90°C.

At time 40,000 seconds, the current load steps down from 150A to 120A, the cell voltage suddenly increases and the stack temperature suddenly decreases. As the result, the controllers ($k_1^{'}$ *and* $k_2^{'}$) will decrease the hydrogen and oxygen flowrates in order to reduce the excess reactants consumption (0.2 mol/s for hydrogen, and 0.23 mol/s for oxygen), and the controller ($k_3^{'}$) will decrease the cooling water about 0.7 mol/s to prevent the stack temperature is too cool and cause of membrane flooding.

The results from Figure 4.6 shows that the three passive controllers for temperature and voltage control are work well under the disturbance is applied to the PEMFC system. The three passive controllers not only maintain the temperature and voltage at their steady state with no any off-sets but the results of temperature and voltage are stable also.

As the membrane humidity (RH) is important for proton exchange membrane fuel cell, this work is also concerning with this issue. The PEMFC can work well at 70% membrane humidity [24]. From Figure 4.6, the system is controlled only the stack temperature and the cell voltage, the membrane humidity ranges between 35%-50%. To address this issue, the membrane humidity control technique is presented in the next section.

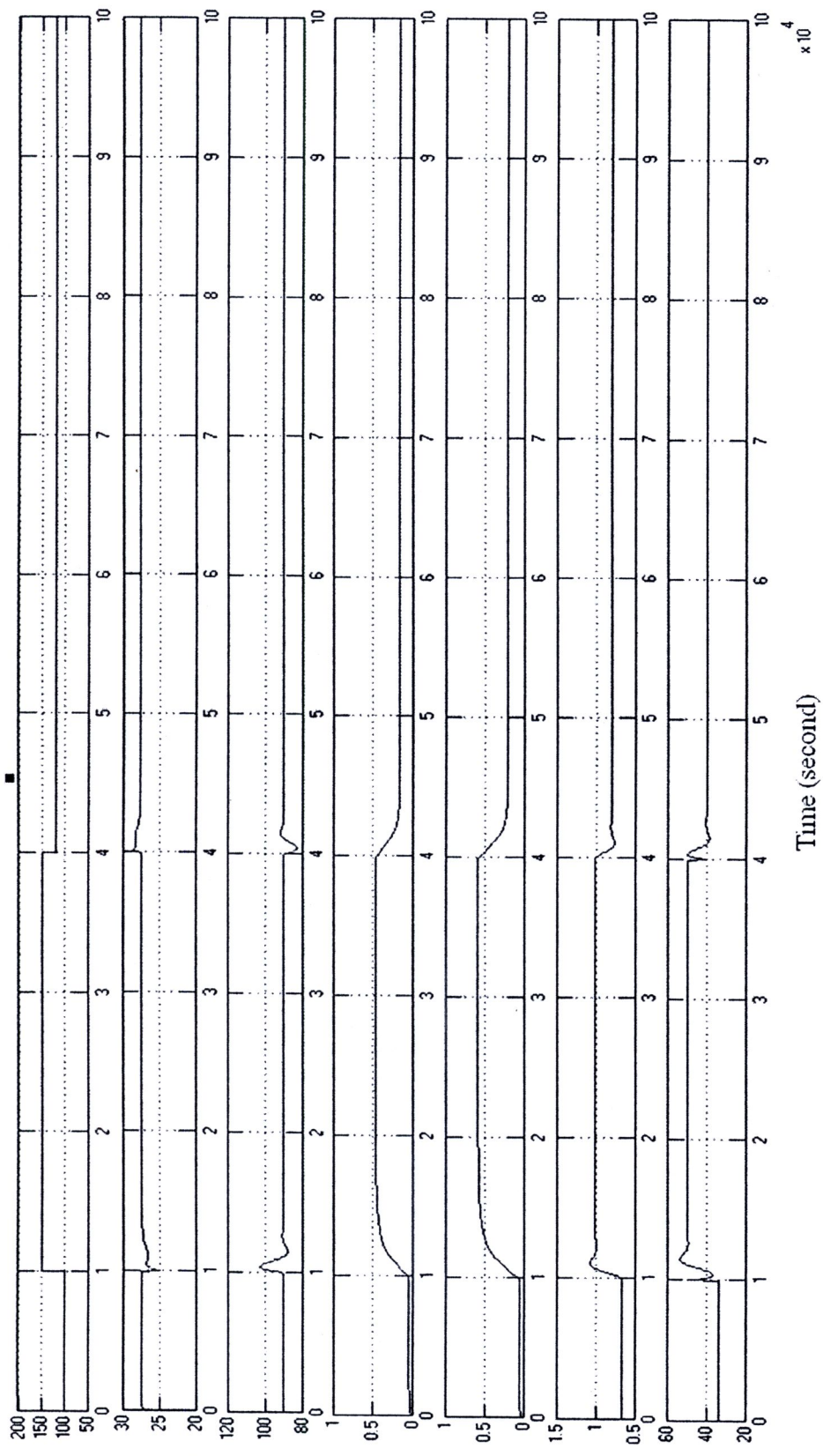

Figure 4.6 The transient response after step change I with T_s *and* V_{stack} controllers

4.5.2 Temperature, voltage and humidity control

Since the membrane humidity (RH) related exactly to the stack temperature of PEMFC, this work presents the humidity control via the cascade control loop because it is most advantageous on applications where the secondary closed loop can include the major disturbance as illustrated in Figure 4.7, which uses the stack temperature set-point signal as the manipulated variable.

In Figure 4.7, the added RH-controller used for humidity control is presented in the circle. In this work, the RH-controller is designed by PI-controller to eliminate the off-set. The parameters of k_c and τ_i for RH-controller are obtained by using Simulink for tuning these values. The suitable values of k_c and τ_i are 1.48 and 0.0005s, respectively. By using these values, the response of membrane humidity gives low overshoot and reaches to it set-point quickly. To handle the membrane humidity problem, the humidity set-point is set to 70% which is sufficiency for proton transportation through membrane. Here is the control strategy for the membrane humidity. The signal from RH-controller acts as the new set point for the stack temperature control. Then, the controller ($k_3^{'}$) will manipulate the cooling water for control both the stack temperature and the membrane humidity. The disturbance variable for this study equals to the previous section, +50A increasing of the current load at time 10,000 seconds, and -30A decreasing at time 40,000 seconds. Figure 4.8 shows the transient responses with temperature-voltage-humidity controllers.

From Figure 4.8, after the current load steps up from 100A to 150A at time 10,000 seconds, and steps down from 150A to 120A at time 40,000 seconds, the response of controllers ($k_1^{'}$ and $k_2^{'}$) are similar to the previous section, increasing the hydrogen and oxygen flowrates to maintain the cell voltage at the steady state value (27.5 Volt) and decreasing the hydrogen and oxygen flowrates to reduce the excess reactants consumption, and maintain the cell voltage at the steady state value, respectively.

For the stack temperature and humidity of PEMFC, after the current load steps up from 100A to 150A at time 10,000 seconds, the stack temperature suddenly increases due to the increasing in electric heat from electrochemical reaction. Since the stack temperature increases, the humidity of membrane drops leading to the proton transportation through membrane will become difficult. As illustrated in Figure 4.8, when the amount of protons can transport through membrane decrease, the cell voltage will also decrease due to the decreasing in the electrochemical reaction. However, the presented control technique can handle both stack temperature and membrane humidity by using the manipulate variable of the RH-controller as the set-point to the stack temperature controller ($k_3^{'}$). Thus, the call from RH-controller is to increase the cooling water about 1.3 mol/s and bring the stack temperature down (75°C), which is around 25 seconds.

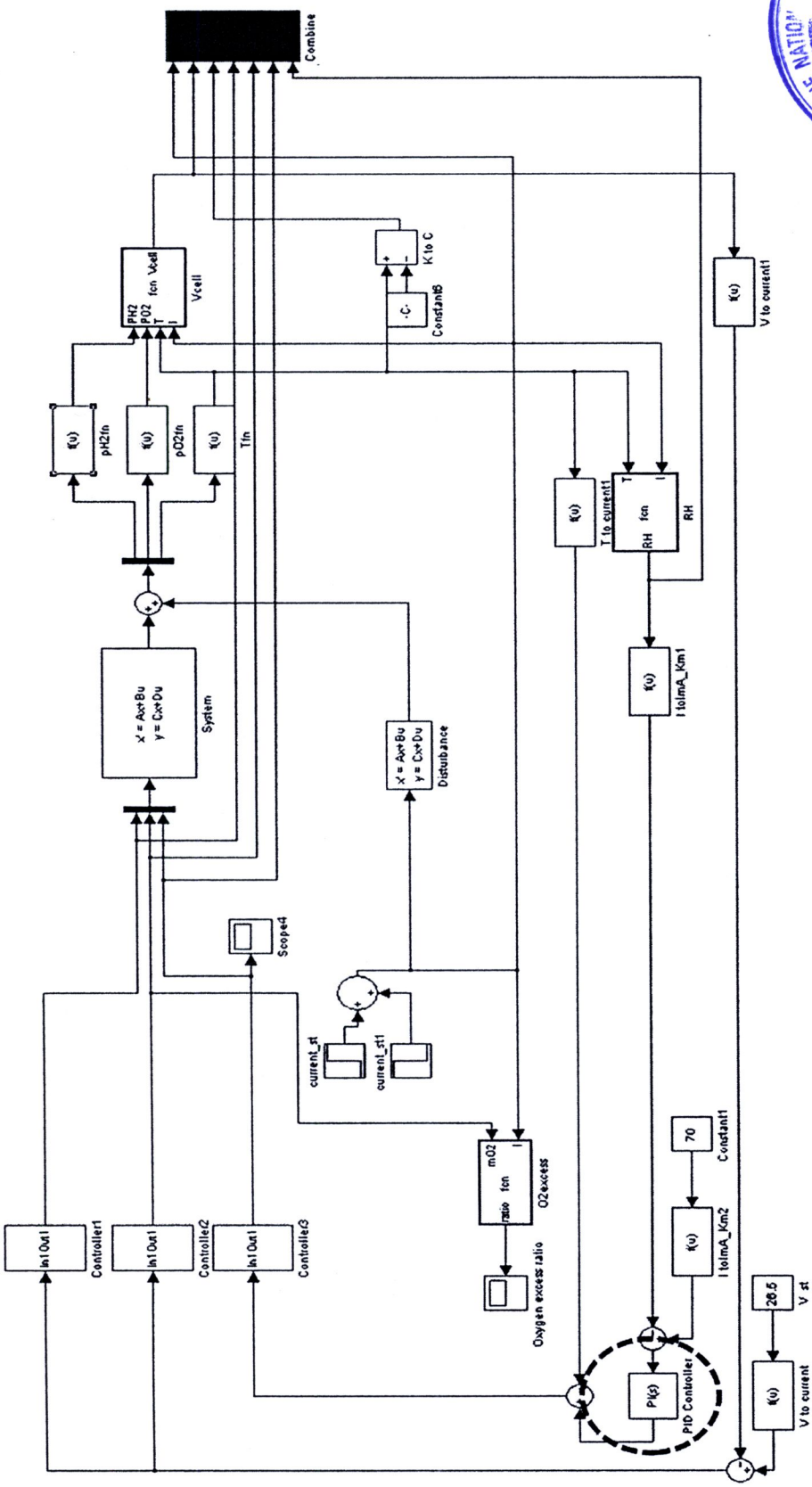

Figure 4.7 The PEMFC model with controller (T_s, V_{stack} *and* RH control)

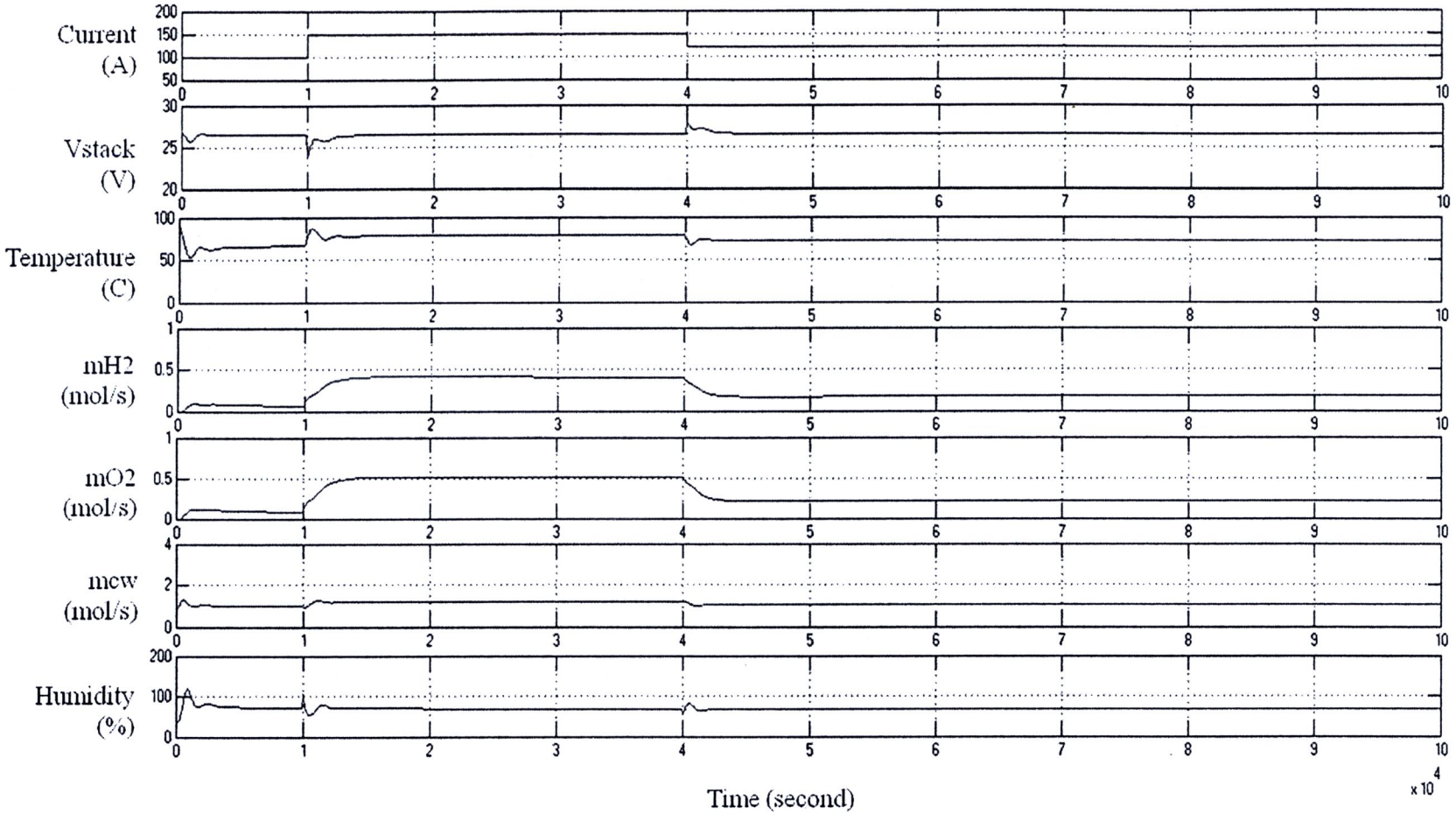

Figure 4.8 The transient response after step change I with T_s, V_{stack} *and* RH controllers

At time 40,000 seconds, the current load steps down from 150A to 120A, the stack temperature decreases because of the decreasing in an electric heat from tan electrochemical reaction. Since the stack temperature decreases, the membrane is cooled down leading to membrane immerse with excess water. To handle this problem, the signal from RH-controller will call the stack temperature controller ($k_3^{'}$) to decrease the cooling water in 50 seconds for maintain the membrane humidity at the desire level (70%).

When comparing the results between these two cases, temperature-voltage control and temperature-voltage-humidity control. The rising time, the time required for temperature, voltage and humidity responses after disturbance is almost the same. In addition, both cases can achieve the cell voltage at it steady state (27.5 Volt) and become stable. However, the second case, temperature-voltage-humidity control is better than the first case because it can achieve not only the membrane humidity but the stack temperature also as represented in Table 4.2. It should be note that although the PEMFC operates at low temperature (75°C), the PEMFC still gives high performance due to the desire level of membrane humidity (70%). The difference of the process responses when the process has and does not has the controllers is illustrated in Table 4.3. After the PEMFC is added with controllers, the responses of the cell voltage, the stack temperature and the membrane humidity are improved significantly. The cell voltage can achieve at 27.5 V which is its maximum value, especially, the stack temperature goes down from 115°C to 75°C. At this point, the PEMFC can be prevented from membrane drying problem reported by 70% of membrane humidity

Table 4.2 The comparing result between two close-loop control

	T-V control	T-V-RH control
Rising time	same	
The cell voltage	27.5 Volt	
The stack temperature	95°C	75°C
The membrane humidity	35%-55%	70%

Table 4.3 The comparing result between open-loop and close-loop control

	Open-loop	Close-loop
The cell voltage	26V	27.5V
The stack temperature	115°C	75°C
The membrane humidity	28%	70%

4.5.3 Temperature, voltage and humidity control with PI-controller

To verify that the passive controller works better than the simple PI-controller, the PEMFC system is controlled by using the PI-controller instead of the passive controller in every control loop. After the load current steps up from 100A to150A at time 10,000 seconds, and steps down from 150A to 120A at 40,000 seconds, the comparing responses of temperature, relative humidity and cell voltage between PEMFC system with passive controller and PI-controller are presented in Figures 4.9.

The results show that after changing the load current at time 10,000 seconds and 40,000 seconds, respectively, the responses of the stack temperature (a), the relative humidity (b) and the cell voltage (c) with PI-controller are more oscillate than passive controller, especially, the relative humidity and the cell voltage. Although the PI-controller can drive the relative humidity and the cell voltage to their set point, the results oscillate for more than 30,000 seconds while the results with passive controller have not. Noticing, at time 10,000 seconds, the cell voltage with PI-controller drops to 24 V due to the oscillation of results. Moreover, the rising time of system with PI-controller is more than passive controller which obviously seen in the cell voltage when the load current is changed. At time 10,000 seconds, the cell voltage with PI-controller uses more than 5,000 seconds to maintain the cell voltage at its set point, while the system with passive controller uses only 1,000 seconds.

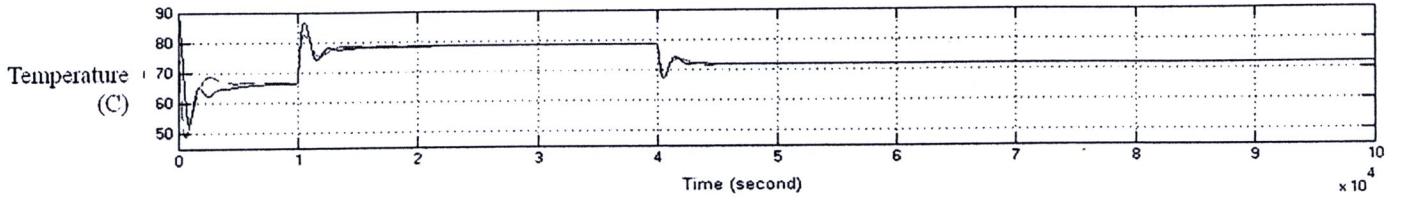

(a) The stack temperature

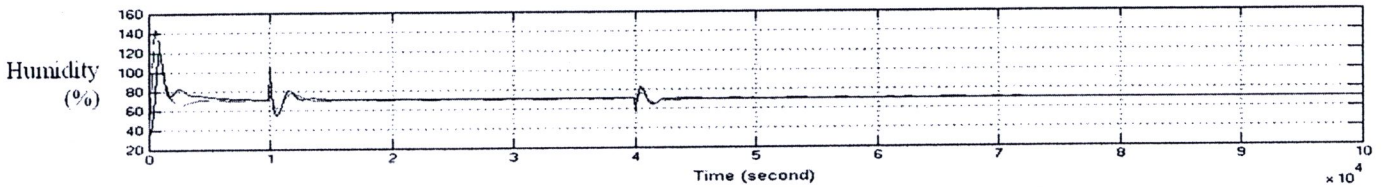

(b) The relative humidity

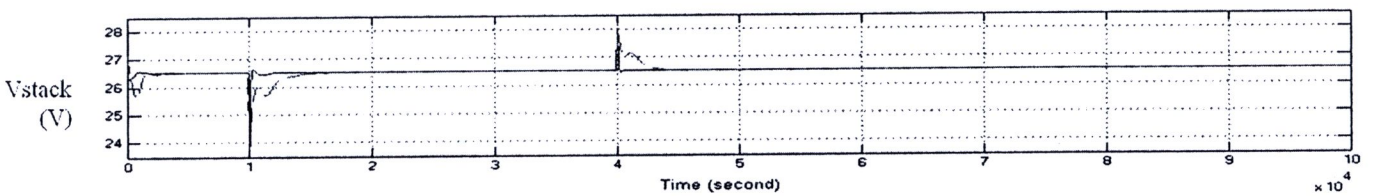

(c) The cell voltage

--------- PI-controller ——— Passive controller

Figure 4.9 The comparing responses between PEMFC system with passive controller and PI-controller

4.5.4 Fault-tolerant control system

Fault-tolerant control system is one of the advantages of passivity concept. In this work, the fault-tolerant is verified by rendering each control loop fails during its operated. There are temperature loop fails $(\dot{m}_{cw} - T)$, oxygen loop fails $(\dot{m}_{O_2} - P_{O_2})$, and hydrogen loop fails $(\dot{m}_{H_2} - P_{H_2})$. Figure 4.10 shows the PEMFC system with temperature loop fails which is presented in the circle and Figure 4.11 shows its transient response.

From Figure 4.11, after the current load steps up from 100A to 150A at time 10,000 seconds, all control variables are driven to their new steady state. The hydrogen and oxygen flowrates increase to 0.45 mol/s and 0.6 mol/s, respectively for maintaining the cell voltage at 27.5 Volt. The cooling water increases to 1.2 mol/s for cooling the stack temperature downs at 80°C. After that, the temperature loop fails to open at time 74,000 seconds. Therefore, the cooling water flows through the process to its maximum value, 1.3 mol/s. Then, more cooling water makes the stack temperature cool downs to 70°C leading to higher membrane relative humidity about 100%. Noticing, the lower stack temperature and the higher membrane humidity cause the cell voltage drops. Therefore, the controller $(k_1^{'} \; and \; k_2^{'})$ will increase hydrogen and oxygen flowrates to maintain the cell voltage at 27.5V. However, noticing that although controller $k_3^{'}$ fails, the overall process can drive to the stable state, and finally the cell voltage can maintain at it set-point with no any off-set.

Figure 4.12-13 show the PEMFC system with oxygen loop fails and its transient response, respectively. After the oxygen loop fails to close (30% open) at time 42,000 seconds, the oxygen flows through the system decreases leading to an increasing of activation loss at cathode side. Therefore, the cell voltage decreases suddenly to its new steady state (25.5V). If comparing the result to Figure 4.4, it is found that the new steady state of the cell voltage when oxygen loop fails is higher than the process without the controllers. This is due to the controllers of the remaining loops (temperature loop and hydrogen loop) are being passive enough for insisting the oxygen loop fail-operational. At time 52,000 seconds, the cell voltage increases to its steady state again (27.5V) by the manipulation of controller $k_1^{'}$ (hydrogen flowrate). However, the failure of controller $k_2^{'}$ (oxygen loop) does not effect to the temperature and also the membrane humidity.

Figure 4.14-15 show the PEMFC system with hydrogen loop fails and its transient response, respectively. After the hydrogen loop fails to close (30% open) at time 47,000 seconds, the responses are the same as PEMFC system with oxygen loop fails. However, after the cell voltage decreases, it increases to steady state faster than that of oxygen loop fail, 1,000 seconds approximately. The failure of controller $k_1^{'}$ (hydrogen loop) does not effect to the temperature and the membrane humidity also.

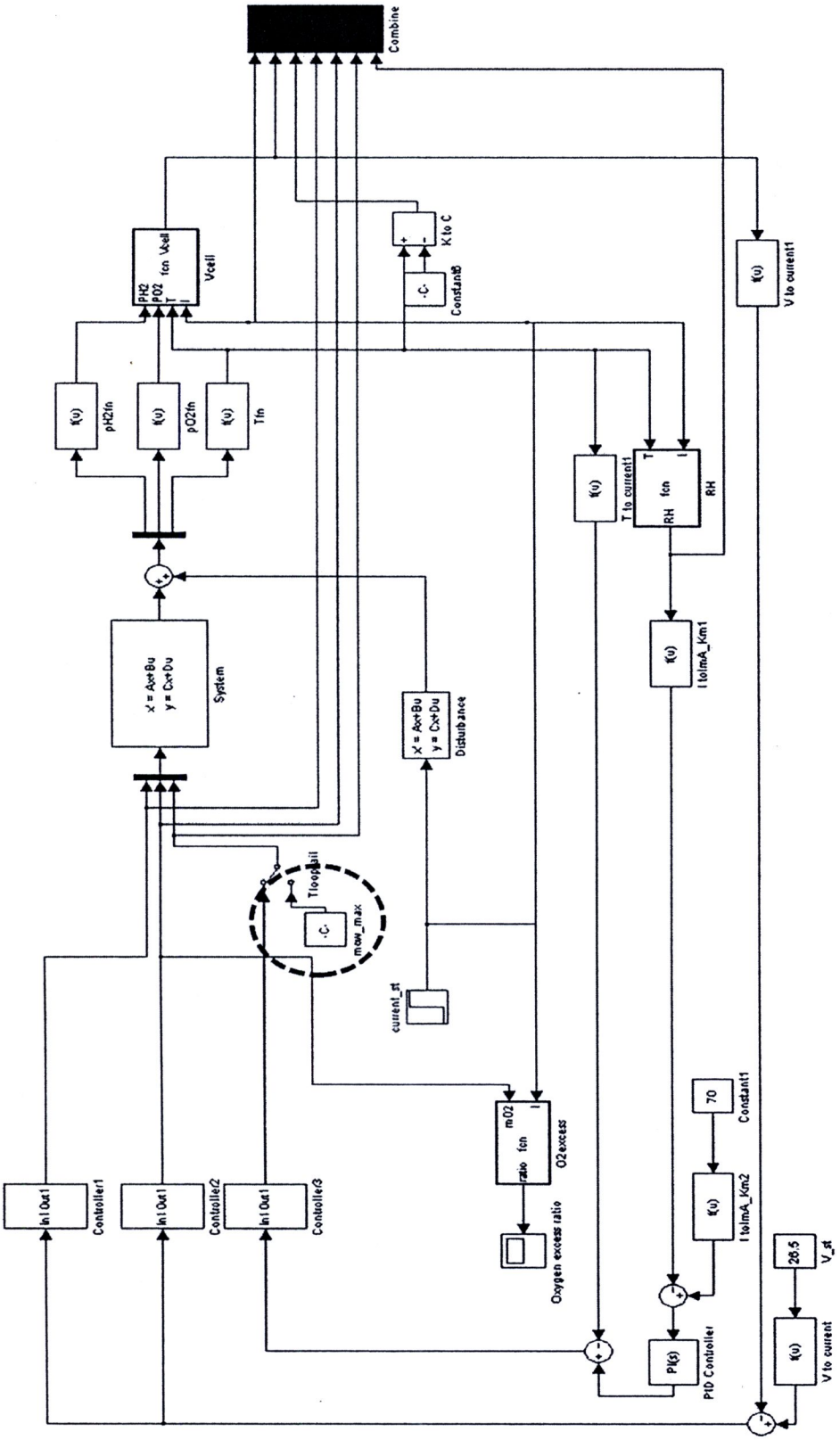

Figure 4.10 The PEMFC system with temperature loop failed

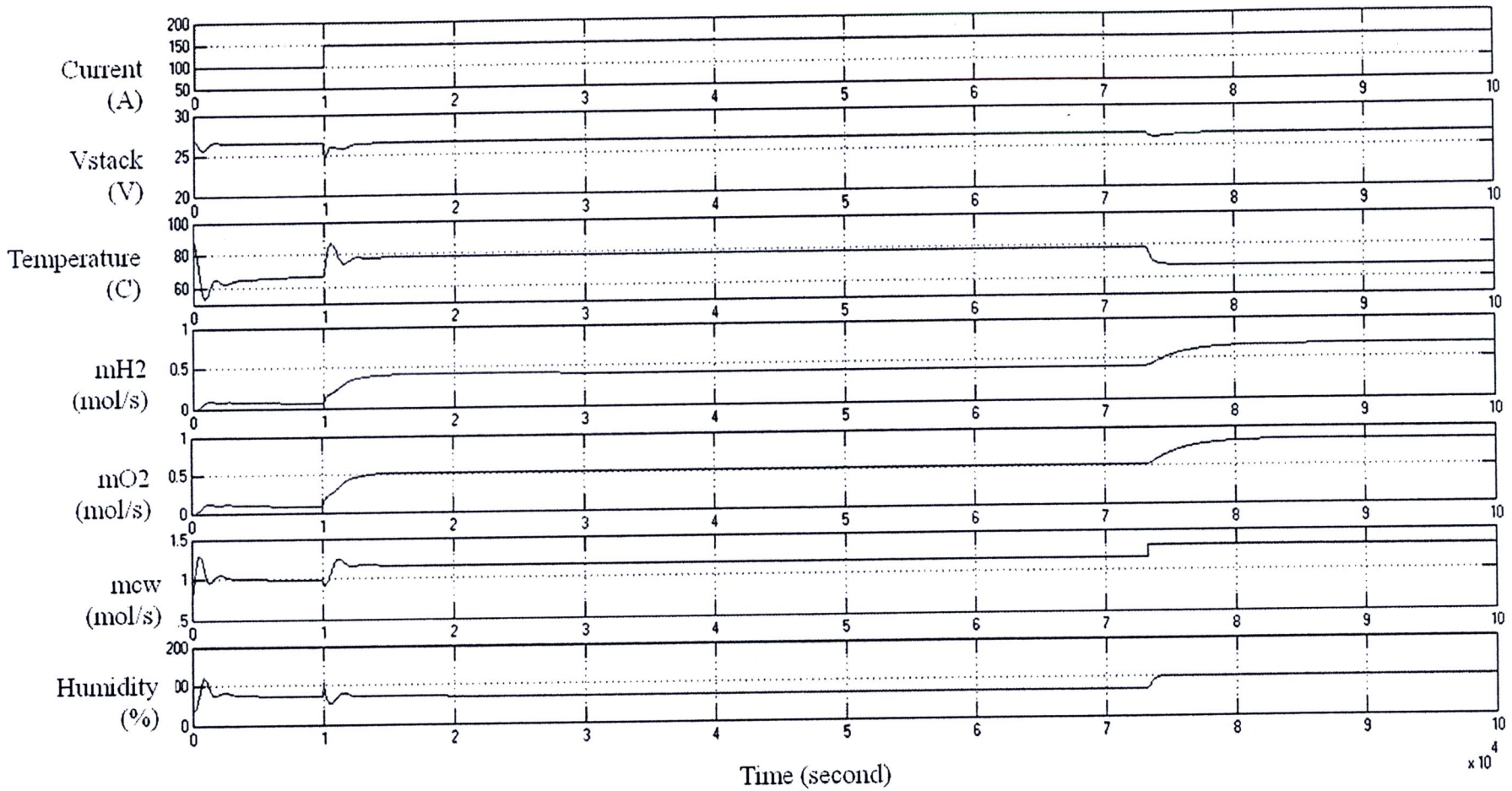

Figure 4.11 The transient response after step change I with temperature loop failed

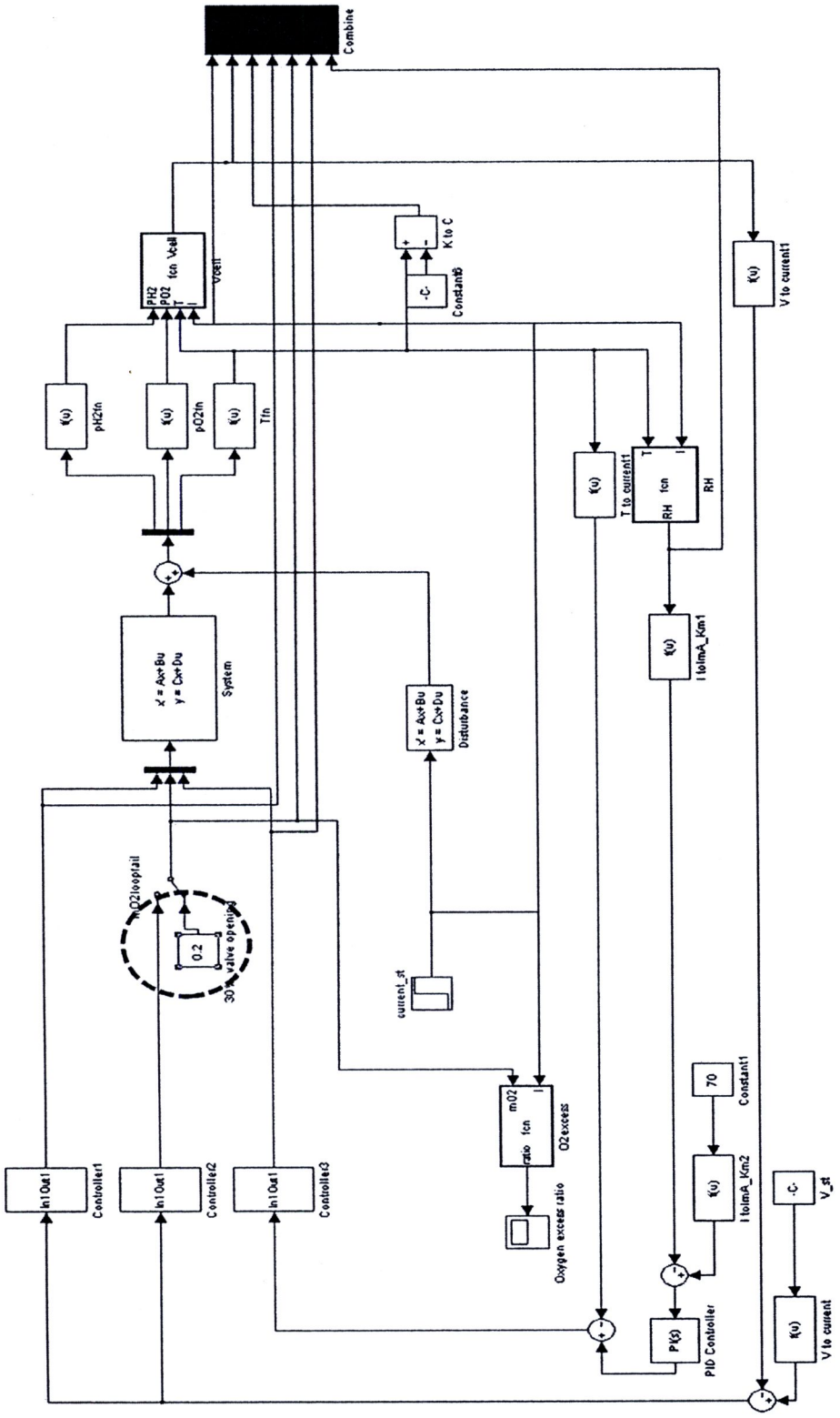

Figure 4.12 The PEMFC system with oxygen loop failed

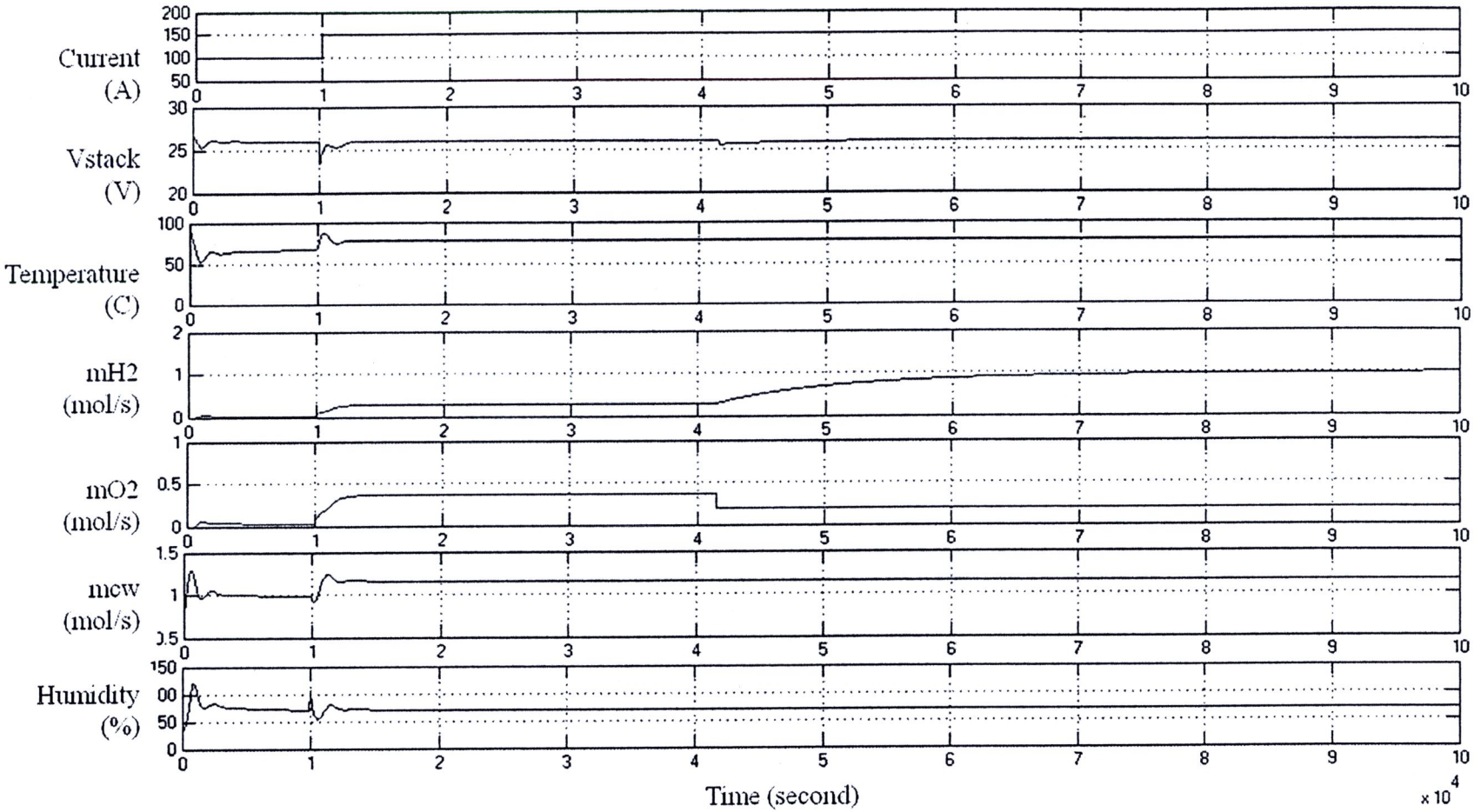

Figure 4.13 The transient response after step change I with oxygen loop failed

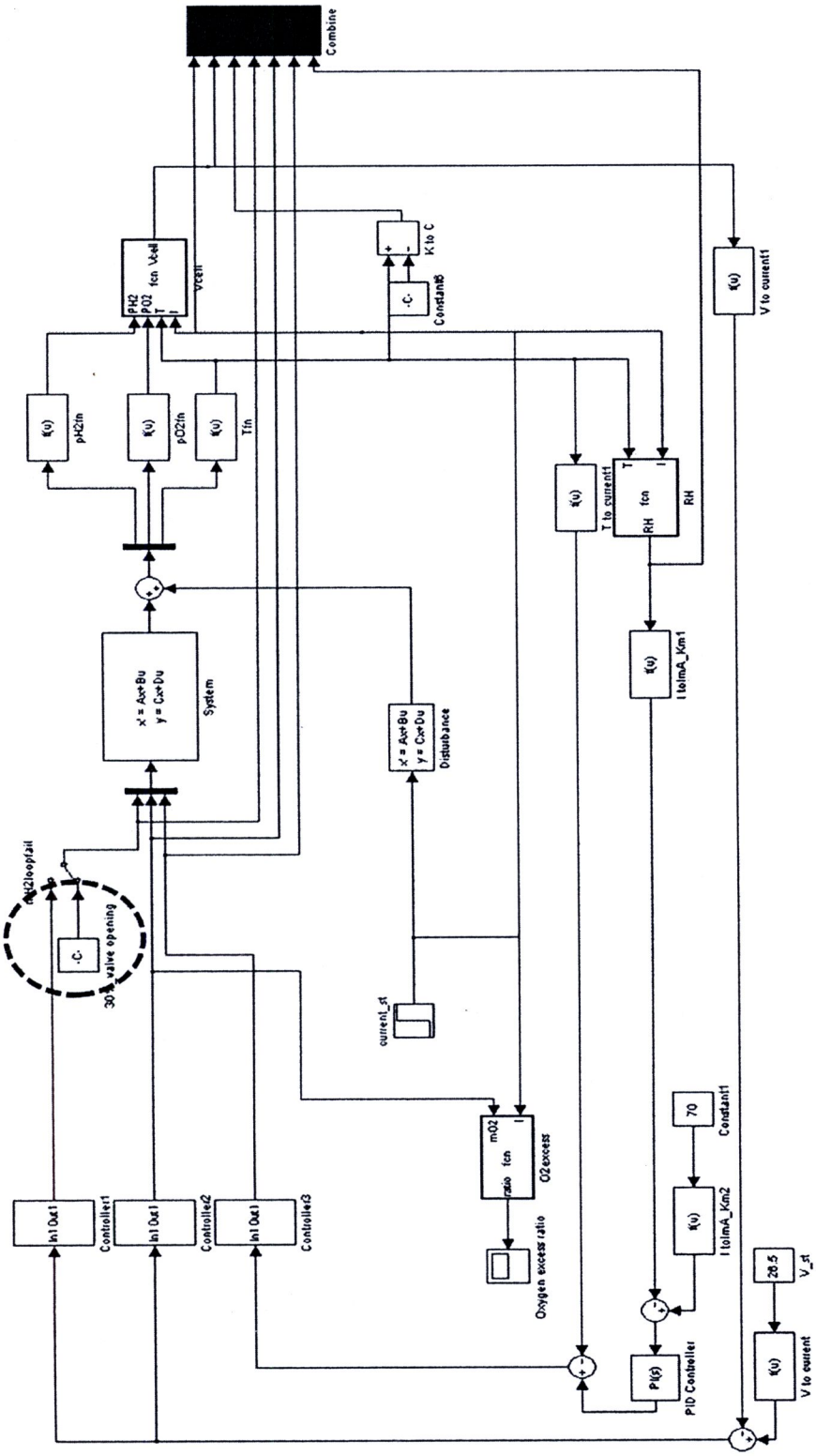

Figure 4.14 The PEMFC system with hydrogen loop failed

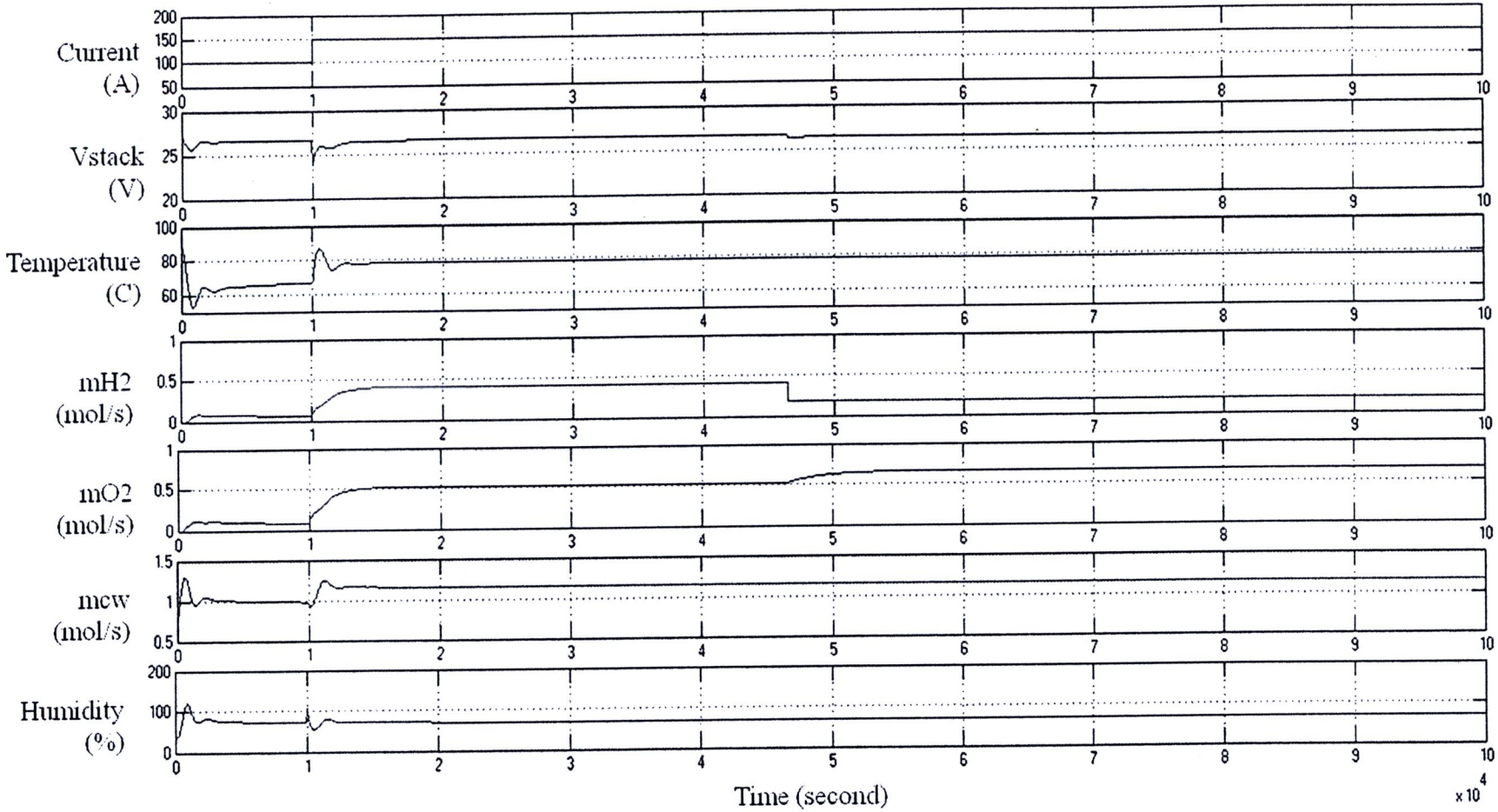

Figure 4.15 The transient response after step change I with hydrogen loop failed

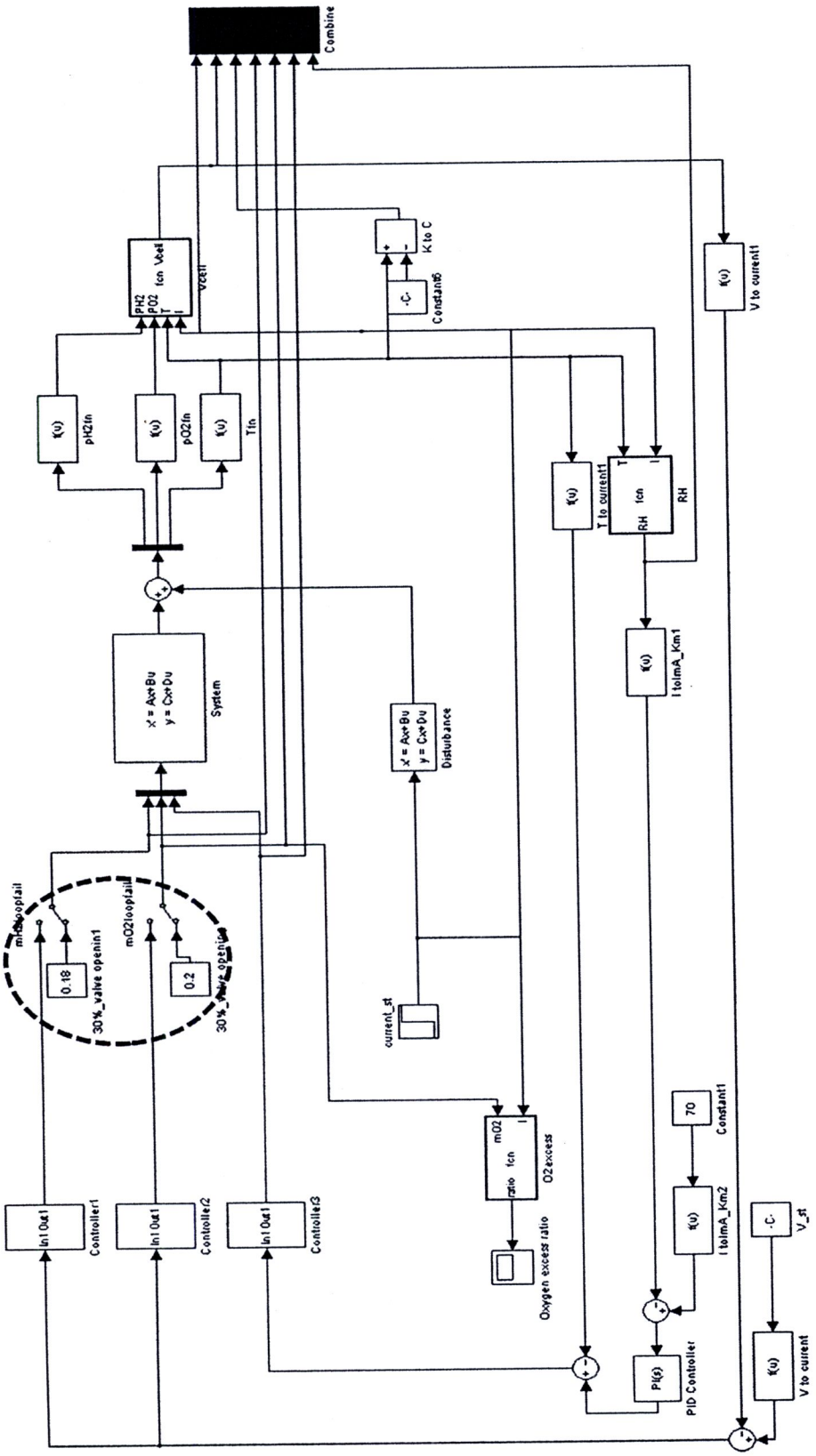

Figure 4.16 The PEMFC system with hydrogen and oxygen loop failed

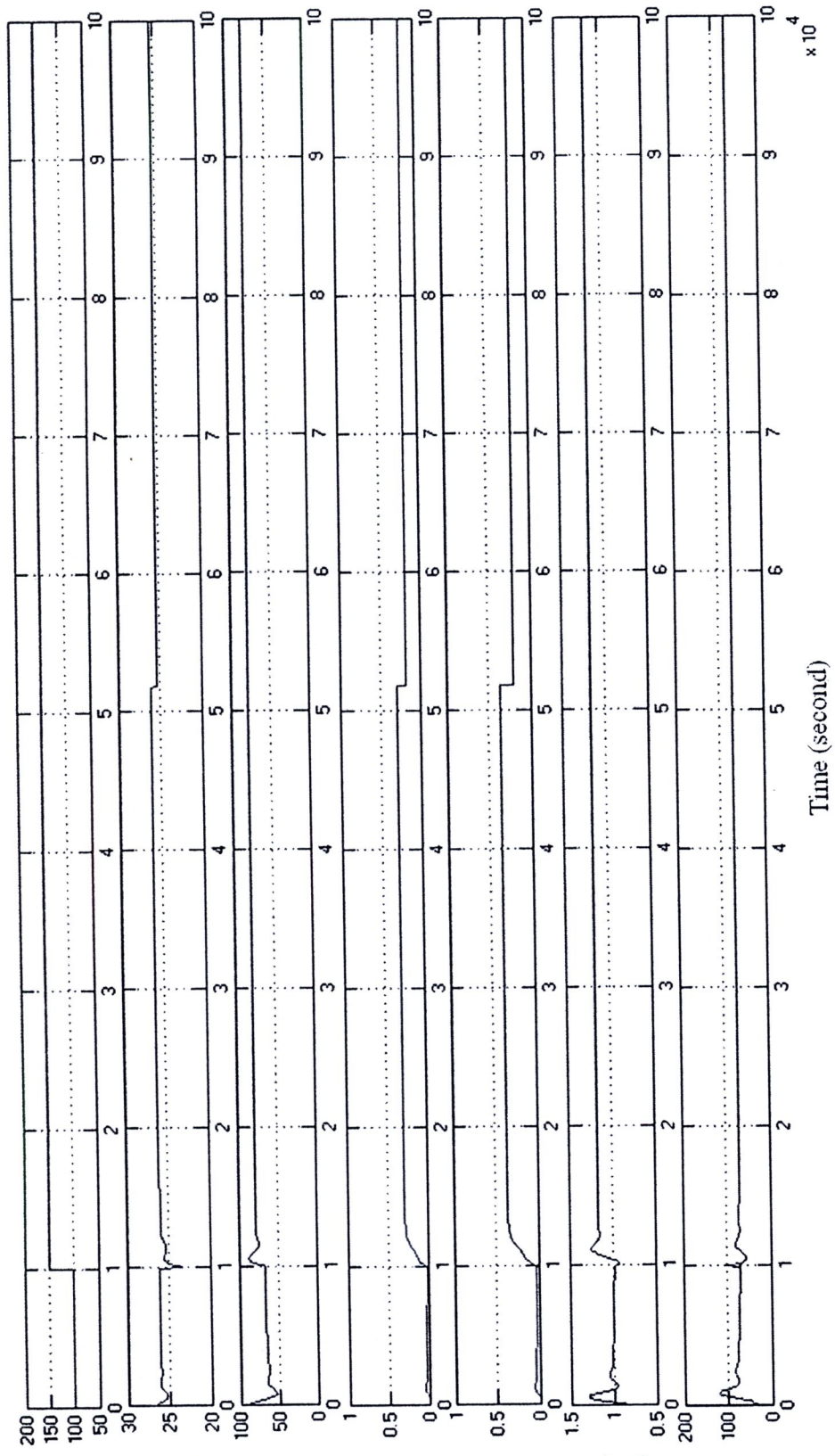

Figure 4.17 The transient response after step change I with hydrogen and oxygen loop failed

The fault-tolerant is not only verified with one loop fails but two loops fail also. In this work, the hydrogen loop and oxygen loop fail to close (30% open) during it is operated. Figure 4.16-17 show the PEMFC system with loops fail and its responses. After the hydrogen and oxygen loop fail to close (30% open) at time 52,000 seconds, the hydrogen and oxygen flow through the system decrease leading to an increasing of activation loss at anode and cathode side. Therefore, the cell voltage decreases suddenly to its new steady state (25.1V). Noticing, after the cell voltage decreases, the remaining controller $k_3^{'}$ does not passive enough in order to drive the cell voltage to its steady state (27.5V). The failure of controller $k_1^{'}$ and $k_2^{'}$ (hydrogen and oxygen loop) do not effect to the temperature and also the membrane humidity. However, it can imply that the stability of fuel cell system is limited to two loops control failed.